phys. stat. sol. (b) **220**, 561 (2000)

Subject classification: 63.22.+m; 73.20.Dx; 78.30.Am; S5; S13

Resonant Raman Scattering in Carbon Nanotubes

C. THOMSEN[1]), P. M. RAFAILOV[2]), H. JANTOLJAK, and S. REICH

Institut für Festkörperphysik, Technische Universität Berlin, Hardenbergstr. 36, D-10623 Berlin, Germany

(Received November 1, 1999)

We present resonant-Raman scattering results on single and multi-walled carbon nanotubes in the range 1.5 to 2.6 eV. In addition to the known resonance of metallic tubes with a maximum at $\approx$1.9 eV we determine the resonance profile of semiconducting single-walled tubes. For a diameter of $d_0 = 1.3$ nm it has a flat minimum between 1.8 and 2.3 eV and a resonance above and below that. For tubes with $d_0 = 1.45$ Å all resonance energies decrease by about 0.1 eV. For multi-walled tubes a monotonic increase in Raman intensity with excitation energy is observed which is explained as a smearing out of the square-root singularities in the electronic density of states of 1D systems.

Introduction The optical properties of carbon nanotubes have become the subject of recent intensive investigations. The combination of a strictly one-dimensional system and the metallic and semiconducting property of a particular tube symmetry is fascinating for basic research. The one-dimensionality leads to a quantum confinement for **k**-vectors perpendicular to the tube axis; parallel to the tube axis **k** can have continuous values [1]. The electronic density of states has singularities characteristic for one dimension, i.e. square-root terms at energies located symmetrically around the Fermi surface and with an energy gap that depends on tube symmetry and diameter [2, 3]. These singularities determine the optical properties of the nanotubes and give rise to resonant processes in the Raman scattering spectra [4, 5].

A nanotube is uniquely specified by its chiral vector $\mathbf{c} = n\mathbf{a}_1 + m\mathbf{a}_2$ along the circumference, $\mathbf{a}_1$ and $\mathbf{a}_2$ forming the elementary cell of graphene. By knowing only the tuple (n, m), e.g., the number of atoms in the unit cell, the point group of the tube can be derived easily. In particular, single-walled nanotubes are metallic if $(n - m)/3$ is an integer and semiconducting otherwise [1].

The vibrational properties of carbon nanotubes have been investigated by a number of groups. The structural similarity to graphite has allowed tentative assignments of vibrational peaks to eigenmodes in the Raman spectra. Polarized spectra, however, have not yet been reported since single crystals or at least highly oriented material have not yet become available. Results on nanotubes enclosed in an oriented matrix [6] and depolarization ratios determined on unoriented samples [7] do not appear to be fully consistent with the symmetries predicted by group theory and leave open the confirmation of the assignments in the Raman spectra. Nevertheless, there is general agree-

[1]) Corresponding author: Tel.: +49-30-314-23187; Fax: +49 30-314-27705; e-mail: thomsen@physik.tu-berlin.de

[2]) Permanent address: Faculty of Physics, University of Sofia, BG-1164 Sofia, Bulgaria.

ment about the physical origin of the two main bands observed in the Raman spectra of single-walled tubes at 150 to 200 cm^{-1}, the so called low-energy mode (LEM), and at $\approx$ 1600 cm^{-1}, the high-energy mode (HEM). The HEM arises from the E_{2g} displacement pattern in graphite and corresponds to a bond-stretching vibration of neighboring carbon atoms. The LEM corresponds to a fully symmetric (A_{1g}) radial breathing-type displacement of the tube with a van-der-Waals contribution from neighboring tubes [8, 9], which does not exist in graphite. In multi-walled tubes there is a single peak at 1583 cm^{-1} corresponding again to the high-energy graphite-like mode; the low-energy mode is generally not seen. A complete group-theoretical analysis of the vibrations in single- and multi-walled nanotubes is given by Damnjanović et al. [10].

When changing the excitation wavelength in single-walled tubes throughout the visible and near infrared strong changes of the relative intensities of the peaks occur in the high-energy region. For 1.5 eV $\leq \hbar\omega_l \leq$ 2.2 eV resonance enhancements of the peaks on the low-energy side of the maximum were observed [5, 11 to 13]. Pimenta et al. normalized their resonance spectra internally, i.e. with respect to the peak intensity of the largest peak outside the resonance at 1592 cm^{-1}. This resonance enhancement was interpreted as due to transitions between the 1D-density of states in metallic nanotubes.

In this paper we report the Raman scattering cross sections of single (SWNT) and multi-walled (MWNT) nanotubes normalized to the scattering intensity of CaF_2 and find the resonance of Pimenta et al. in SWNT qualitatively confirmed. However, in single-walled tubes the peak at 1592 cm^{-1} undergoes a resonance as well, showing that it may not be used for normalization. We calculate the joint density of states for both semiconducting and metallic single-walled nanotubes and compare them with the normalized Raman spectra. For two SWNT samples with a different mean diameter the resonance maximum shifts, as expected, inversely proportional with tube diameter. In addition, we report preliminary resonance measurements on multi-walled tubes, which in accordance with the calculated density of states, show a monotonic increase of the scattering efficiency in the range considered.

Experimental Multi-walled nanotubes were produced by the arc-discharge method from graphite, the SWNT from a mixture of metallic catalysts (Ni and Y) and graphite. The latter are organized in ropes with a triangular lattice structure [14, 15]. For the investigation of the diameter dependence we selected two samples with different mean tube diameters. From TEM images the majority of SWNT diameters d was found to be 1.1 to 1.5 nm and 1.2 to 1.7 nm in the two samples, following a Gaussian-like distribution with mean values $d_0 = 1.3$ nm and 1.45 nm and a halfwidth of about 0.1 nm.

The Raman spectra of the single-walled nanotubes were recorded on a Dilor XY 800 spectrometer equipped with a liquid-nitrogen cooled CCD. The multi-walled measurements were performed under a microscope with a Labram spectrometer. An Ar^+/Kr^+-ion-gas laser and a Ti:sapphire laser were used for excitation energies between 1.59 and 2.55 eV and an excitation intensity below 500 W/cm^2. All measurements were performed at room temperature in the backscattering geometry. For normalization purposes we also recorded the intensity of the optical mode of CaF_2 taken under the same experimental conditions. The optical properties of CaF_2 are constant over the examined energy range (1.59 to 2.55 eV) [16]. A necessary correction to the resonant excitation profiles when comparing to the joint density of states is to account for the varying optical penetration depth of the nanotube sample, which determines the scattering vol-

ume. From optical measurements [3] we found the absorption length to decrease approximately by a factor of two when varying the excitation energy from 1.6 to 2.6 eV. The excitation profiles of the nanotube samples were thus obtained as a Raman scattering efficiency normalized to the scattering efficiency of the CaF_2 phonon.

Results and Discussion In Fig. 1 we show the Raman spectra in the high-energy region of two SWNT with different diameters and MWNT. Going from bottom to top we decreased the excitation energy. In Fig. 1a we find that the spectra excited with 2.54 eV are dominated by the peak at 1592 cm^{-1}, which corresponds to the type of spectra usually reported in the literature. At this energy the spectra depend only little on the diameter of the tube [17], the relative intensities of the two peaks do not change much. In the maximum of the metallic resonance near $\hbar\omega_l = 1.92$ eV we see that the low-energy side of the spectra is strongly enhanced relative to the peak at 1592 cm^{-1}. Note that the two diameters produce now a significant difference: for the larger diameter ($d_0 = 1.45$ nm) the low-energy peak is weaker than the 1592 cm^{-1} peak, while for the smaller diameter ($d_0 = 1.3$ nm) it is stronger. This behavior is expected since the density of states maximum shifts to higher energies for smaller tube diameters. At the lowest energy ($\hbar\omega_l = 1.61$ eV) the spectra look again similar to those above the resonance, the two diameters again not showing a noticeable difference. In Fig. 1b the multi-walled spectra recorded for the same excitation energies are shown. The spectra look alike,

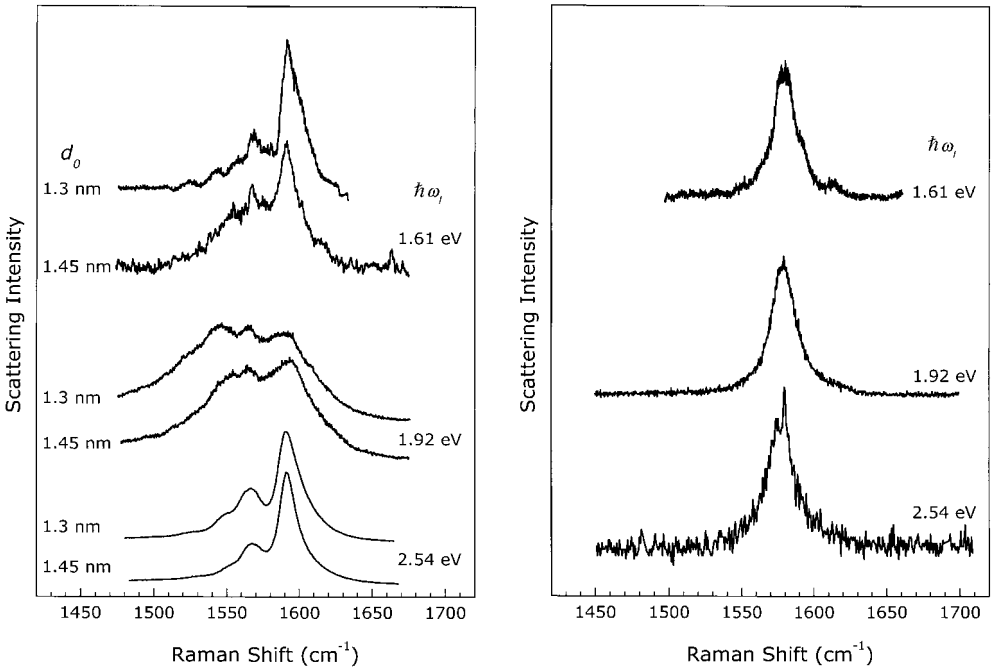

Fig. 1. Raman spectra at three different excitation energies. a) The high-energy mode of two single-walled nanotube samples with different diameters d_0. b) The high-energy mode of a multi-walled nanotube sample. Note how the relative intensities in the SWNT spectra change with energy, while there is no apparent excitation-energy dependence in MWNT

demonstrating the absence of such sharp resonances as found in the single-walled species.

We will now show that the difference in resonance behavior is due to the different electronic structure of single- and multi-walled tubes. The resonance energies of a given SWNT are determined by the separation between the mirror image spikes in the 1D electronic density of states and are thus diameter dependent [2]. The transitions contributing to the resonance are those from a singularity in the i-th valence band to one in the i-th conduction band [4, 18]. Transitions with $i \neq j$ occur with a much smaller probability for symmetry reasons [18], and we neglect their influence. Multi-walled nanotubes, on the other hand, consist of concentric tubes with subsequentially increasing diameter. In the approximation that interactions between these tubes can be neglected, we consider the electronic density of states (EDOS) of an MWNT to be the sum of the corresponding single-walled tubes. The large outer diameters of a typical MWNT ($d_{\text{out}} = 7.5$ nm) compared to SWNTs ($d_0 = 1.3$ nm) cause many spikes in the EDOS at low energies. This generates a quasi continuous density of states and results in a loss of a pronounced resonance behavior in the MWNT spectra.

Semiconducting SWNTs with diameters similar to those of our samples have three pairs of such singularities within ± 1.5 eV of the Fermi level [1, 19] separated by about 0.5 to 0.7 eV. Metallic SWNTs exhibit only one pair of spikes in this energy range with a gap of 1.5 to 2.2 eV accounting for the metallic resonance. These predictions were confirmed by combined scanning tunneling microscopy and spectroscopy (STM and STS) [20, 21]. In particular, the separation of the first pair of singularities for metallic SWNTs with diameters 1.2 to 1.4 nm was found to be 1.7 to 2.0 eV.

The energy gap in a single nanotube E_{ii} is inversely proportional [2] to the tube diameter d and equal to $E_{ii} = 2ia_{\text{C-C}}\gamma_0/d$ where for metallic tubes $i = 3, 6, \ldots$ and for semiconducting tubes $i = 1, 2, 4, 5, 7, \ldots$ Here $a_{\text{C-C}} = 1.42$ Å is the nearest-neighbor distance of the C-atoms and γ_0 the nearest-neighbor electronic overlap integral. The γ_0 values reported range from 2.5 eV to 3.14 eV. STM experiments [21] yield a γ_0 value of 2.7 eV and resonance Raman experiments [5] 2.95 eV. Despite the uncertainty in γ_0 a typical diameter distribution will result in broad bands of electronic transitions for both semiconducting and metallic SWNT and a complete smearing out of these transitions for MWNT. For the examined energy range the different E_{ii} in SWNT imply the existence of windows where the incident light cannot resonantly enhance the vibrational modes in metallic or semiconductivity tubes, respectively.

We now estimate the resonance Raman profile of both SWNT and MWNT by summing up the Raman matrix elements over the joint density of states involved in the process in a similar way as was done in Ref. [13]. The matrix element $K(\hbar\omega_{\text{l}})$ of the Raman process is [22]

$$K(\hbar\omega_{\text{l}}) = \frac{M_i H_{ij} M_j}{(\hbar\omega_{\text{l}} - \hbar\omega_i - i\gamma_i)\,(\hbar\omega_{\text{s}} - \hbar\omega_j - i\gamma_j)}\,, \tag{1}$$

where $\omega_{\text{l}}(\omega_{\text{s}})$ are the frequencies of the incident (scattered) light, $\omega_{i,j}$ are the frequencies of the resonant electronic transitions with matrix elements $M_{i,j}$, γ_i is the damping factor of the i-th transition and H_{ij} is the electron–phonon Hamiltonian matrix element. To obtain the Raman cross section this matrix element is summed over all possible $\omega_{i,j}$ and then squared [22, 23]. Because of the quasi one-dimensionality of the electronic density of states this sum can be converted into an integral over the joint DOS

(JDOS). To obtain a convenient expression for the JDOS in the examined energy region we use the approximation of Mintmire et al. [24] to calculate a universal density of states of SWNT. We find that in a particular tube the i-th pair of energy bands (a valence and a conduction band symmetric with respect to the Fermi level) introduces into the JDOS, $J(E)$, a term of the form $a_{C-C}E/d\gamma_0 \sqrt{E^2 - E_{ii}^2}$ whenever $E > E_{ii}$. This is a good appoximation provided $a_{C-C}/d \ll 1$, which is satisfactorily fulfilled by our samples ($a_{C-C}/d \approx 0.1$).

Weighting the JDOS expression by a Gaussian diameter distribution ($d_{min} \leq d \leq d_{max}$) for SWNT we obtain the JDOS of all tubes in a SWNT sample as follows:

$$J^{SWNT}(E) \propto \sum_i \sum_{d=d_{min}}^{d_{max}} \frac{a_{C-C}E}{d\gamma_0 \sqrt{E^2 - {E_{ii}}^2}} \exp\left[-\left(\frac{d-d_0}{\sqrt{2}\sigma}\right)^2\right], \quad (2)$$

where d_0 is the mean diameter of the SWNT in the sample and σ the Gaussian width parameter. In our experiment on SWNT only terms with $i = 1$, 2, and 4 for the semiconducting tubes and $i = 3$ for the metallic tubes contribute significantly.

The JDOS curves of the SWNT samples with mean diameters 1.3 nm are plotted in Fig. 2a. The JDOS curve has a resonance-like shape modulated by the square-root singularities of the individual tubes. The Raman intensity profile should exhibit the same resonance behavior as the matrix elements $M_{i,j}$ provided H_{ij} can be regarded as constant over the resonance range. For the small-diameter tubes with strongly pronounced 1D-singularities in the density of states, we approximate the JDOS of such

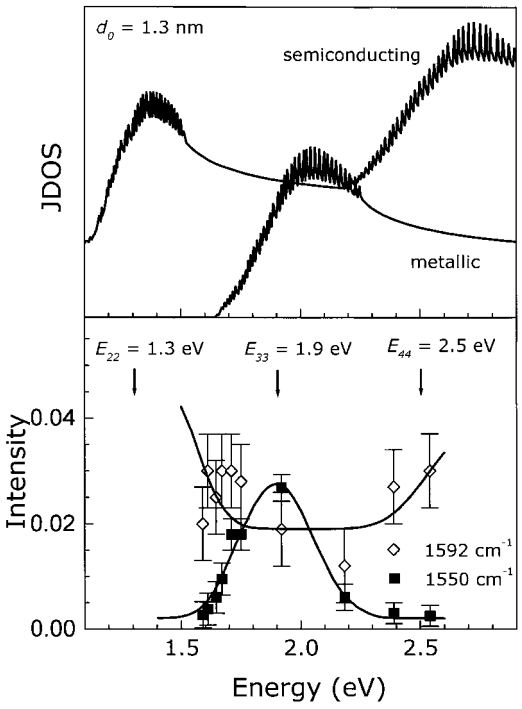

Fig. 2. a) Calculated joint density of states for semiconducting and metallic tubes and b) normalized resonant intensities of the Raman peaks at 1550 and 1592 cm^{-1} of a single-walled nanotube sample with mean diameter d_0 = 1.3 nm. Also shown is the fit to the data using Eq. (4)

tubes as

$$J^{\mathrm{SWNT}}(E) \approx \sum_i \sum_{d=d_{\min}}^{d_{\max}} (a_0/d)\ \delta(E - E_{ii}) \exp\left[-\left(\frac{d-d_0}{\sqrt{2}\sigma}\right)^2\right], \tag{3}$$

where again i is appropriately chosen for semiconducting and metallic SWNT. Integration yields the excitation profiles of both semiconducting and metallic single-walled tubes:

$$I^{\mathrm{SWNT}}(\hbar\omega_{\mathrm{l}}) = \sum_i \sum_{d=d_{\min}}^{d_{\max}} \frac{1}{d^2} \frac{A \exp\left[-\left(\frac{d-d_0}{\sqrt{2}\sigma}\right)^2\right]}{[(E_{ii} - \hbar\omega_{\mathrm{l}})^2 + \gamma_{\mathrm{e}}^2/4]\,[(E_{ii} - \hbar\omega_{\mathrm{l}} + \hbar\omega_{\mathrm{ph}})^2 + \gamma_{\mathrm{e}}^2/4]}. \tag{4}$$

Here A is a normalization factor, $\hbar\omega_{\mathrm{ph}} = 0.199$ eV and 0.194 eV are the energies of the created phonons, and the damping factor γ_{e} is taken to be the same for the bands considered. We have included the diameter distribution as a Gaussian exponent with a halfwidth $\approx$0.1 nm. Equation (4) is similar to the one used by Pimenta et al. [5], but differs in the weighting factor d^{-2}. In Fig. 3a we show the joint density of states for a larger-diameter single-walled nanotube. It is clearly seen that the resonance energies of semiconducting and metallic tubes shift to lower energies and that the spacing between the spikes becomes smaller. Our expression thus properly accounts for the stronger resonant enhancement of tubes with smaller diameter.

Equation (4), with the appropriate indices distinguishing semiconducting and metallic tubes, was fitted to the Raman intensities of the peaks at $\omega_{\mathrm{ph}} \approx 1592$ cm^{-1} and 1550 cm^{-1} corrected and normalized to CaF_2 as described. The adjusted parameters are the nearest-neighbor overlap integral γ_0 and the damping factor γ_{e}. The results are shown in Fig. 2b together with the experimental data. Apparently the resonance profiles of the two peaks are well described by the two predicted types of resonances. The metallic resonance has a maximum due to E_{33} at 1.9 eV and drops

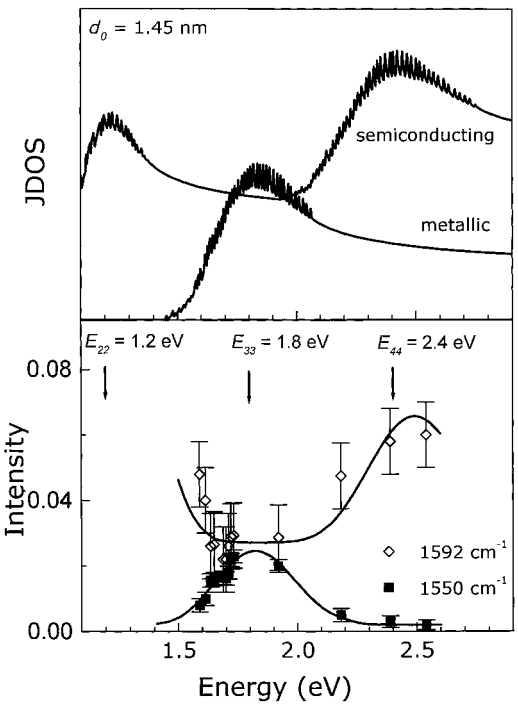

Fig. 3. Like Fig. 2 but for a larger mean diameter single-walled nanotube sample (d_0 = 1.45 nm)

off sharply for energies above and below that (closed symbols). The semiconducting resonances, according to the expression for $E_{ii} = 2ia_{C-C}\gamma_0/d$ with $\gamma_0 = 2.9$ eV from the fit, have maxima at $E_{22} = 1.3$ eV and at $E_{44} = 2.5$ eV, just outside the range considered here. The experimental data for the 1592 cm^{-1} peak confirm the increasing Raman cross sections (open symbols in Fig. 2b) and allow for a satisfactory description of both resonance profiles. In Fig. 3b we show the corresponding results for the larger tube-diameter sample ($d_0 = 1.45$ nm). The metallic resonance is indeed shifted to lower energy; $E_{33}(d_0 = 1.45\,\text{nm}) = 1.8$ eV is the energy in the maximum. The resonance energies of the 1550 cm^{-1} peak shift to $E_{22} = 1.2$ eV and to $E_{44} = 2.4$ eV ($\gamma_0 = 2.9$ eV), correspondingly.

For multi-walled tubes we proceeded similarly to obtain the joint density of states, except that the Gaussian distribution in diameters used in Eq. (2) is replaced by a fixed number of diameters given by the inner and outer diameter of the MWNTs. We sum over all diameters incrementing in steps of the wall-to-wall separation in MWNT ($\approx 2 \times 3.4$ Å) from d_{in} to d_{out}. We chose $d_{in} = 4$ nm and $d_{out} = 18$ nm in accordance with the TEM pictures of our multi-walled tubes and found the result to be nearly independent of the exact values. Thus

$$J^{MWNT}(E) \propto \sum_i \sum_{d=d_{in}}^{d_{out}} \frac{a_{C-C}E}{d\gamma_0\sqrt{E^2 - E_{ii}^2}}\,, \tag{5}$$

the index i this time is chosen such that all energies in the range considered (≤ 3 eV) are included. As d increases, the index successively increases as well. Figure 4a shows the joint density of states for an MWNT with the above parameters. It is seen to increase linearly, i.e., the spikes in the density of states are entirely washed out by the averaging process in the multi-walled tubes. Figure 4b shows the experimental results, again normalized to the intensity of the CaF_2 phonon. We find a similar monotonic increase of the Raman scattering intensity, in rough agreement with the joint density of states. This is similar to the behavior of graphite [12] although we might expect some modulation of the Raman profile due to the inner tubes of the MWNT. Measurements with more closely spaced excitation energies are planned to resolve this issue.

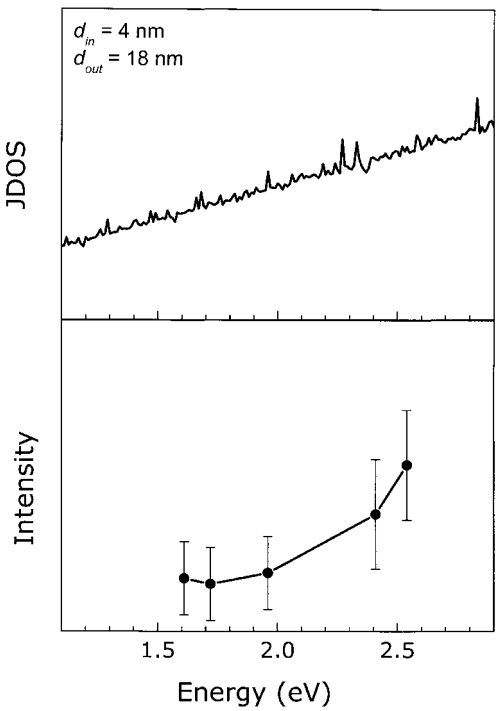

Fig. 4. a) Joint density of states of a multi-walled nanotube sample and b) normalized resonant intensities of the Raman peak at 1583 cm^{-1}

Conclusions From resonant Raman profiles determined in single-walled nanotubes of two different mean diameters and in multi-walled tubes we were able to confirm the one-dimensionality of the electronic density of states in nanotubes. The metallic SWNTs show pronounced resonances ($E_{22} = 1.9$ eV for the smaller d and 1.8 eV for the larger d). The semiconducting resonances appear as shoulders in our spectra; their energy is found at $E_{22} = 1.3$ eV and 2.5 eV ($d_0 = 1.3$ nm) and about 0.1 eV below that for $d_0 = 1.45$ nm. The inverse diameter dependence of the energy of the singularities in the density of states is confirmed. We obtained the carbon–carbon electronic overlap integral $\gamma_0 = 2.9 \pm 0.2$ eV and the broadening parameter $\gamma_e = 0.065 \pm 0.01$ eV from a fit to the data, in good agreement with results obtained by other experimental techniques. In multi-walled nanotubes the Raman cross sections increase with excitation energy, in rough agreement with the linear dependence of the calculated density of states for such tubes.

Acknowledgements We thank P. Bernier and C. Journet for providing us with the nanotube samples. We gratefully acknowledge valuable discussions with A.R. Goñi. P.M.R. acknowledges a research fellowship from the Deutscher Akademischer Austauschdienst (Germany).

References

[1] M. S. DRESSELHAUS, G. DRESSELHAUS, and P. C. EKLUND, Science of Fullerenes and Carbon Nanotubes, Academic Press, New York 1996.
[2] J. C. CHARLIER and PH. LAMBIN, Phys. Rev. B **57**, R15037 (1998).
[3] H. KATAURA, Y. KUMAZAWA, Y. MANIWA, I. UMEZU, S. SUZUKI, Y. OHTSUKA, and Y. ACHIBA, Synth. Metals **103**, 2506 (1999).
[4] A. M. RAO, E. RICHTER, S. BANDOW, B. CHASE, P. C. EKLUND, K. A. WILLIAMS, S. FANG, K. R. SUBBASWAMY, M. MENON, A. THESS, R. E. SMALLEY, G. DRESSELHAUS, and M. S. DRESSELHAUS, Science **275**, 187 (1997).
[5] M. A. PIMENTA, A. MARUCCI, S. A. EMPEDOCLES, M. G. BAWENDI, E. B. HANLON, A. M. RAO, P. C. EKLUND, R. E. SMALLEY, G. DRESSELHAUS, and M. S. DRESSELHAUS, Phys. Rev. B **58**, R16016 (1998).
[6] H.D. SUN, Z.K. TANG, J. CHEN, and G. LI, Solid State Commun. **109**, 365 (1999).
[7] C. THOMSEN, S. REICH, P.M. RAFAILOV, and H. JANTOLJAK, phys. stat. sol. (b) **214**, R15 (1999).
[8] C. THOMSEN, S. REICH, A. R. GOÑI, H. JANTOLJAK, P. M. RAFAILOV, I. LOA, K. SYASSEN, C. JOURNET, and P. BERNIER, phys. stat. sol. (b) **215**, 435 (1999).
[9] U. D. VENKATESWARAN, A. M. RAO, E. RICHTER, M. MENON, A. RINZLER, R. E. SMALLEY, and P. C. EKLUND, Phys. Rev. B **59**, 10928 (1999).
[10] M. DAMNJANOVIC, I. MILOSEVIC, T. VUKOVIC, and R. SREDANOVIC, Phys. Rev. B **60**, 2728 (1999). I. MILOSEVIC and M. DAMNJANOVIC, Phys. Rev. B **47**, 7805 (1993).
[11] M. SUGANO, A. KASUYA, K. TOHJI, Y. SAITO, and Y. NISHINA, Chem. Phys. Lett. **292**, 575 (1998).
[12] A. KASUYA, M. SUGANO, and C. HORIE, Phys. Rev. B **57**, 4999 (1998).
[13] P. M. RAFAILOV, H. JANTOLJAK, and C. THOMSEN, Phys. Rev. B **61**, 16179 (2000).
[14] C. JOURNET, W. K. MASER, P. BERNIER, A. LOISEAU, M. LAMY DE LA CHAPELLE, S. LEFRANT, P. DENIARD, R. LEE, and J. E. FISCHER, Nature (London) **388**, 756 (1997).
[15] C. JOURNET and P. BERNIER, Appl. Phys. A **67**, 1 (1998).
[16] I. S. GRIGORIEV and E. Z. MEILIHOV (Eds.), Physical Quantities, Energoatomizdat, Moscow 1991.
[17] A. KASUYA, Y. SASAKI, Y. SAITO, K. TOHJI, and Y. NISHINA, Phys. Rev. Lett. **78**, 4434 (1997).
[18] E. RICHTER and K. R. SUBBASWAMY, Phys. Rev. Lett. **79**, 2738 (1997).
[19] R. SAITO, T. TAKEYA, T. KAMURA, G. DRESSELHAUS, and M. S. DRESSELHAUS, Phys. Rev. B **57**, 4145 (1998).
[20] T. W. ODOM, J. L. HUANG, P. KIM, and C. M. LIEBER, Nature (London) **391**, 62 (1998).
[21] J. W. G. WILDÖER, L. C. VENEMA, A. G. RINZLER, R. E. SMALLEY, and C. DEKKER, Nature (London) **391**, 59 (1998).
[22] R. M. MARTIN and L. M. FALIKOV, in: Light Scattering in Solids I, Topics of Applied Physics, Vol. 8, Ed. M. CARDONA, Springer-Verlag, New York 1983.
[23] P. YU and M. CARDONA, Fundamentals of Semiconductors, Springer-Verlag, New York 1996.
[24] J. W. MINTMIRE and C. T. WHITE, Phys. Rev. Lett. **81**, 2506 (1998).